



# Edge Sensors for Segmented Telescopes

Chris Shelton

ExEP Tech Colloquium Jan 23 2017

LUVOIR Subgroup Meeting Jan 27 2017



**Jet Propulsion Laboratory**  
California Institute of Technology

# Keck, TMT, E-ELT

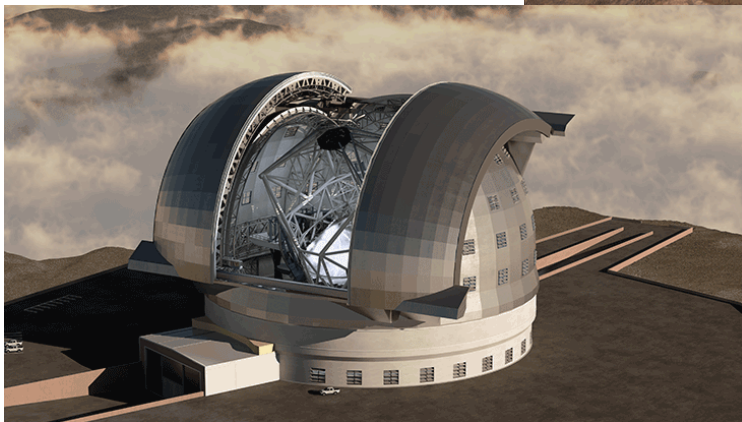
**Keck**  
2 x 10m  
36 Segments  
168 Edge sensors  
Capacitive, interleaved  
Height/tilt output



**TMT**  
30m  
492 Segments  
2772 Edge sensors  
Capacitive, face-on  
Height/tilt and gap outputs



**E-ELT**  
39m  
798 Segments  
4524 Edge sensors,  
Inductive, face-on  
Height/tilt, gap and shear outputs



# Control Geometry

## Implications for Edge Sensors

# Segmented Mirror Active Control Geometry

Three actuators move each segment as a rigid body, in tip, tilt and piston.

Edge sensors report on the relative position of neighboring segments.

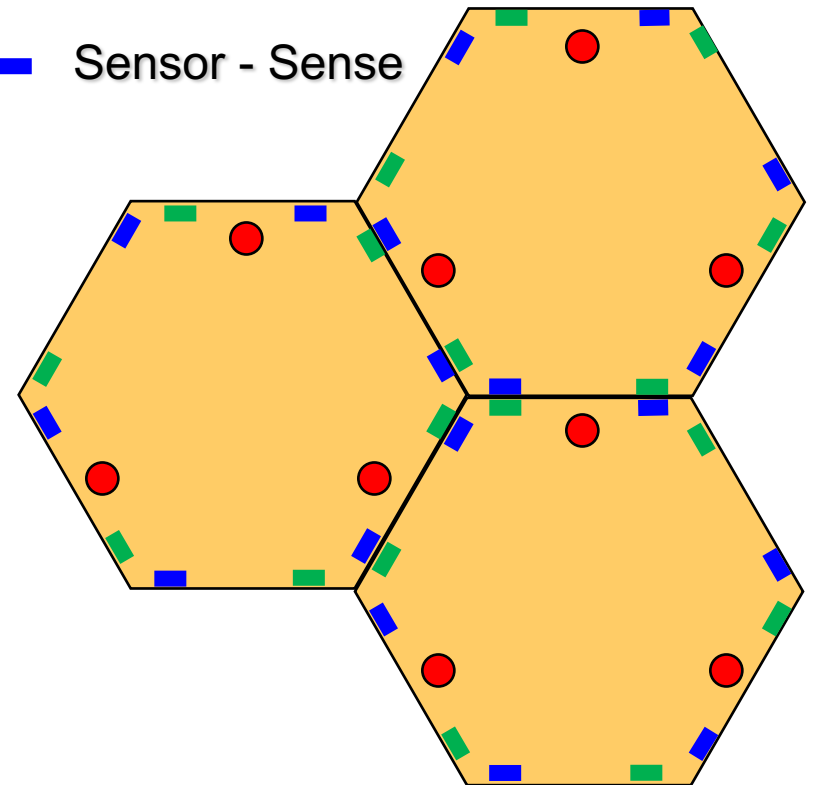
A sensor has a drive half on one segment and a sense half on the other side of the gap between segments.

Keck, TMT and E-ELT sensors have a “height” output proportional to a combination of height and dihedral angle. The ratio of height to angle sensitivity is called the effective lever arm, or  $L_{eff}$ .

TMT and E-ELT sensors have a “gap” output giving a measure of the gap between the sensor halves.

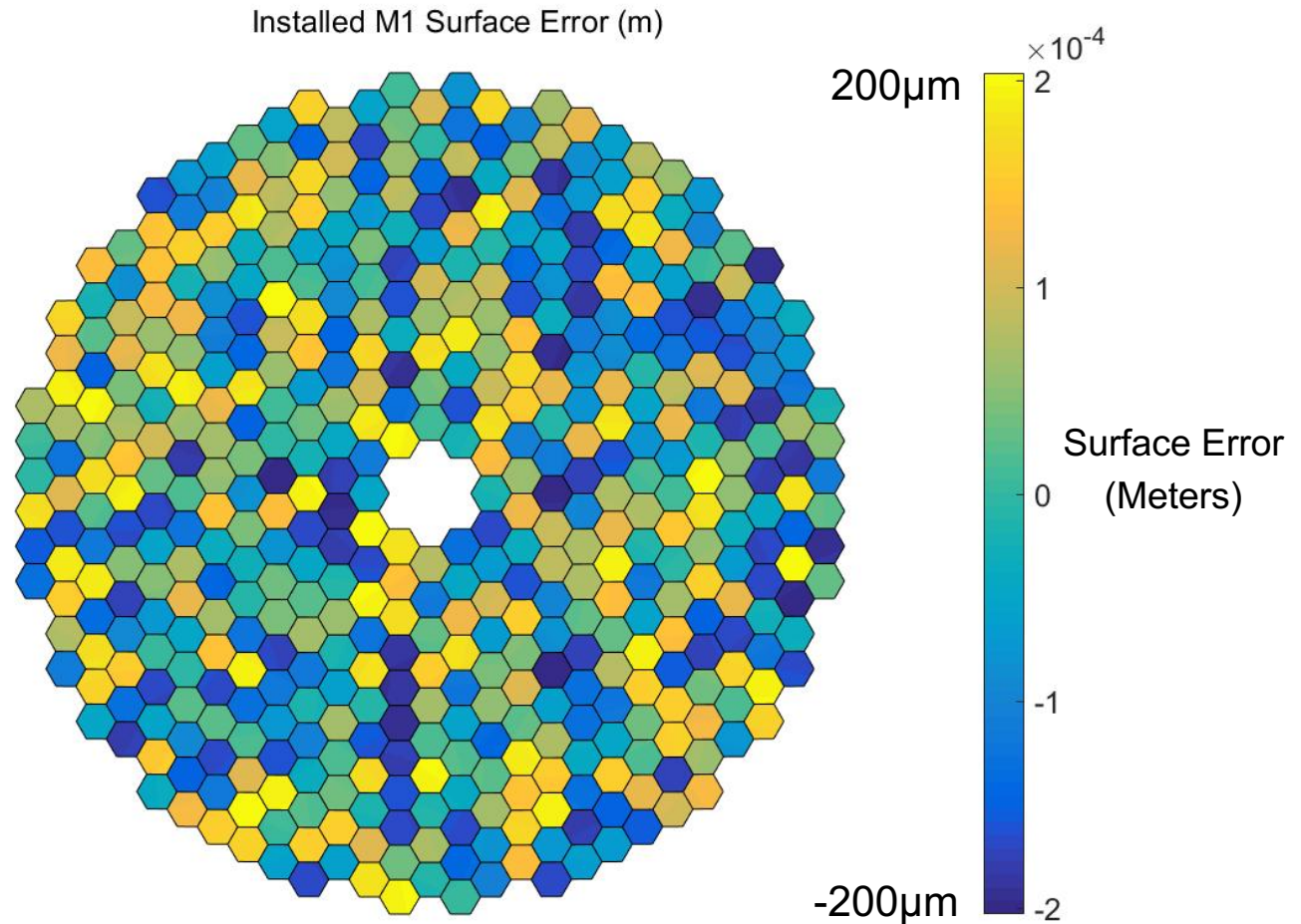
E-ELT sensors provide a “shear” output proportional to segment-segment displacement along a common edge. TMT computes shears from gaps.

- Actuators
- Sensor - Drive
- Sensor - Sense



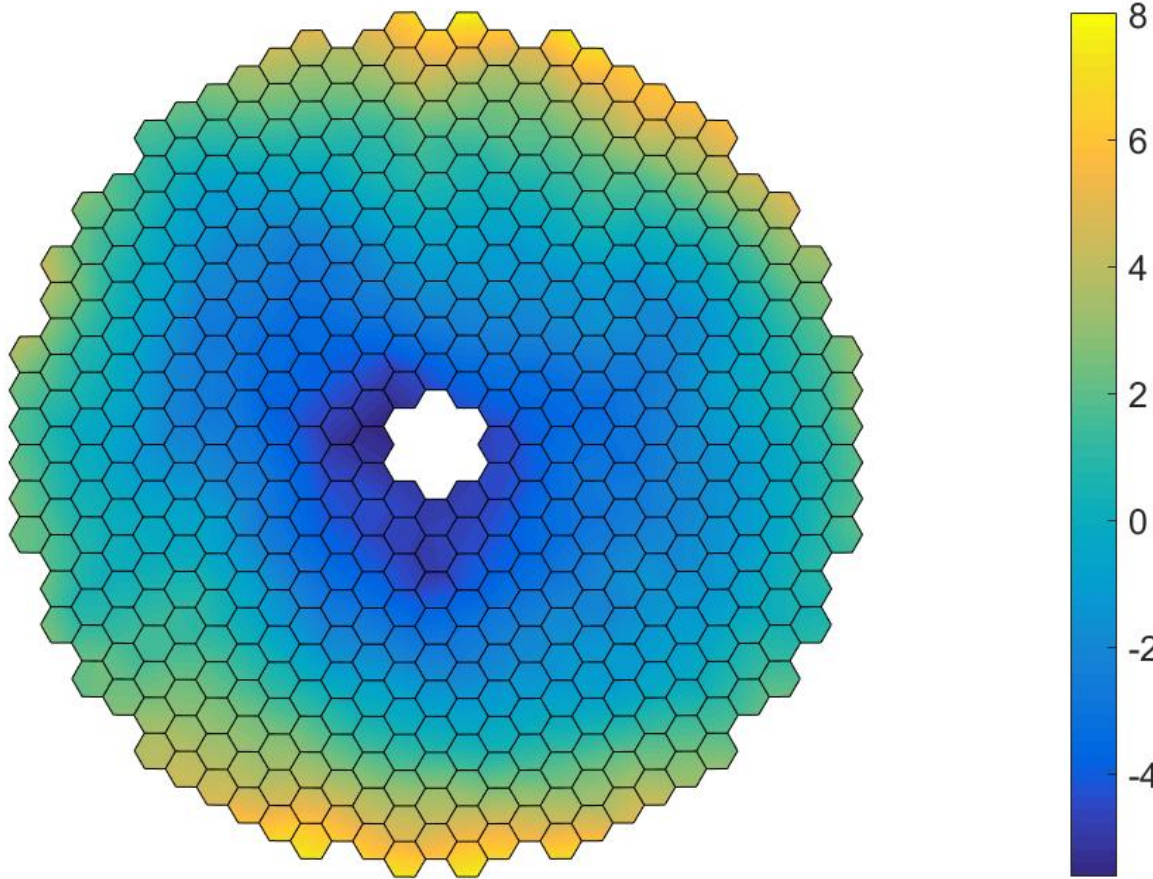
# Surface Error at Initial Segment Installation

Installation tolerance in z is  $200\mu\text{m}$



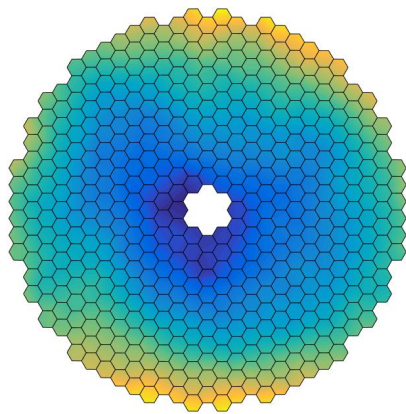
# OPD (in mm!), M1CS initial turn-on

M1 is made smooth, but with large low-frequency errors

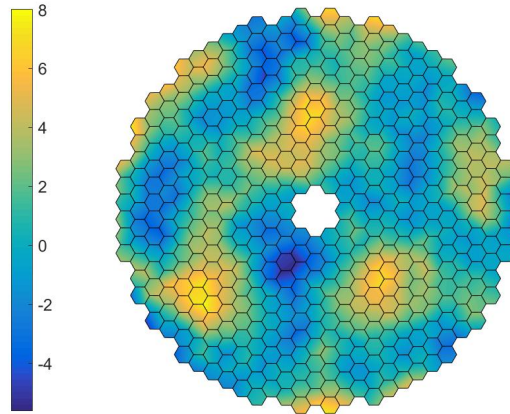


# External Input from a WFS can help

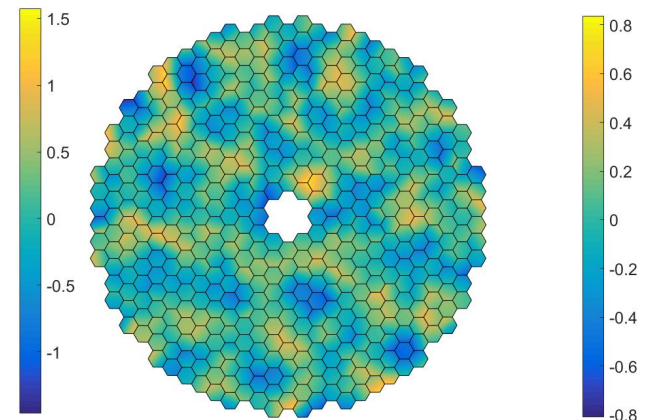
These figures give some idea of how much error is in low Zernike modes



No external input  
-5 to +8 mm OPD



15 Zernikes corrected  
(TMT AGWFS)  
-1.3 to +1.5 mm OPD



60 Zernikes corrected  
(TMT NFIRAOS)  
-0.8 to +0.8 mm OPD

Sensor height installation error = 27  $\mu\text{m}$  rms.

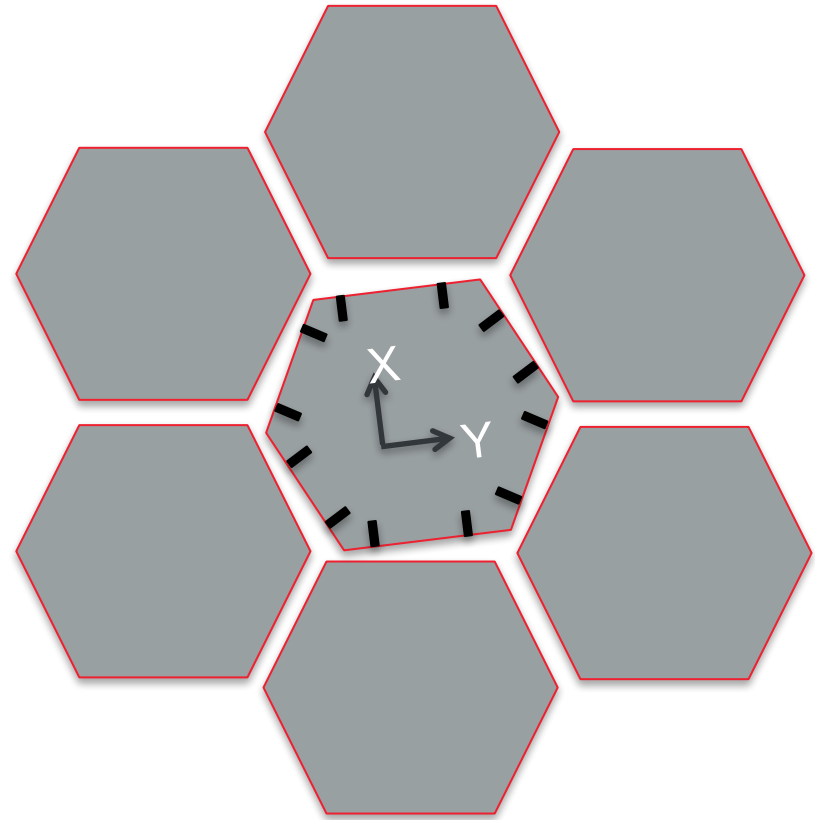
AGWFS = Acquisition, Guiding, and Wavefront Sensing

NFIRAOS = Narrow Field Infrared Adaptive Optics System

# Segment Clocking

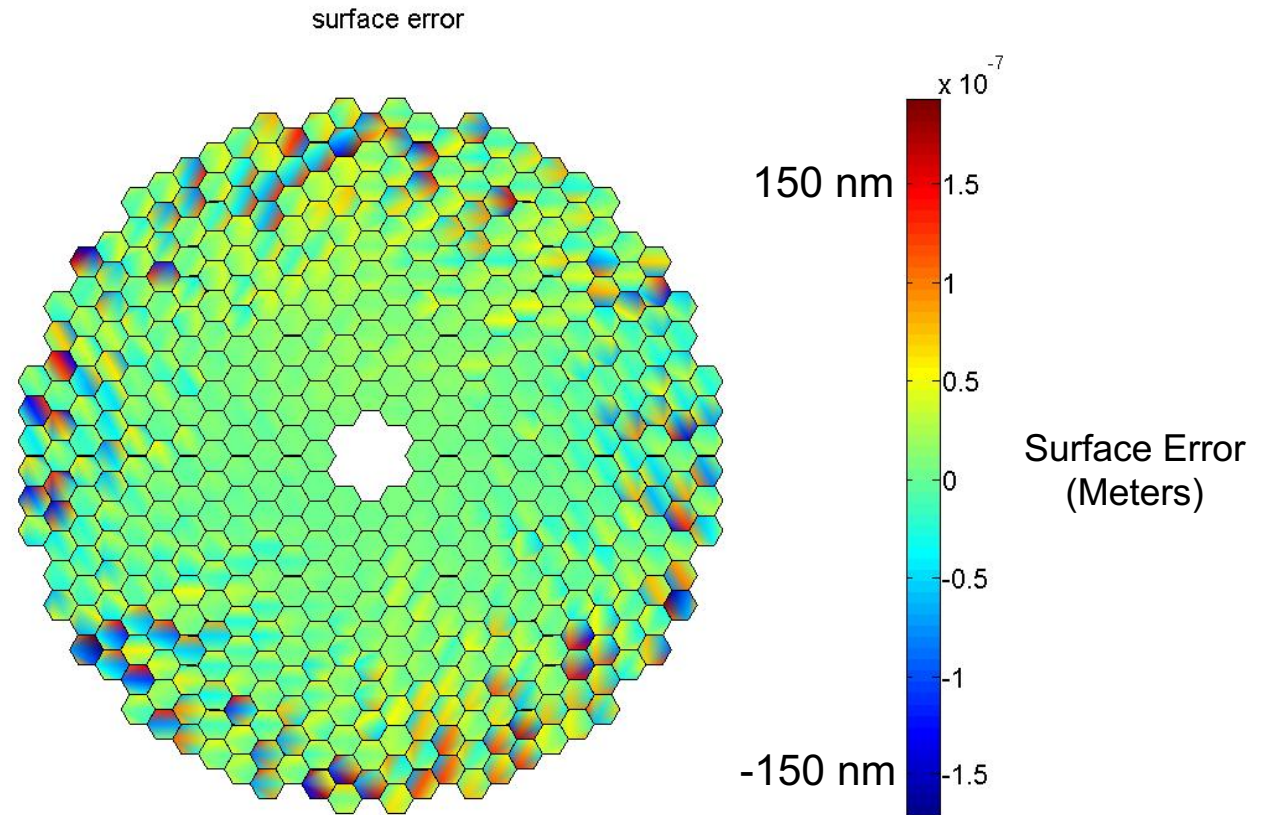
Segment clocking of outer segments creates astigmatism which is corrected by warping the segment.

For TMT, segments are warped at one zenith angle and temperature, and not warped again until segment replacement.



# The Impact of Segment Clocking

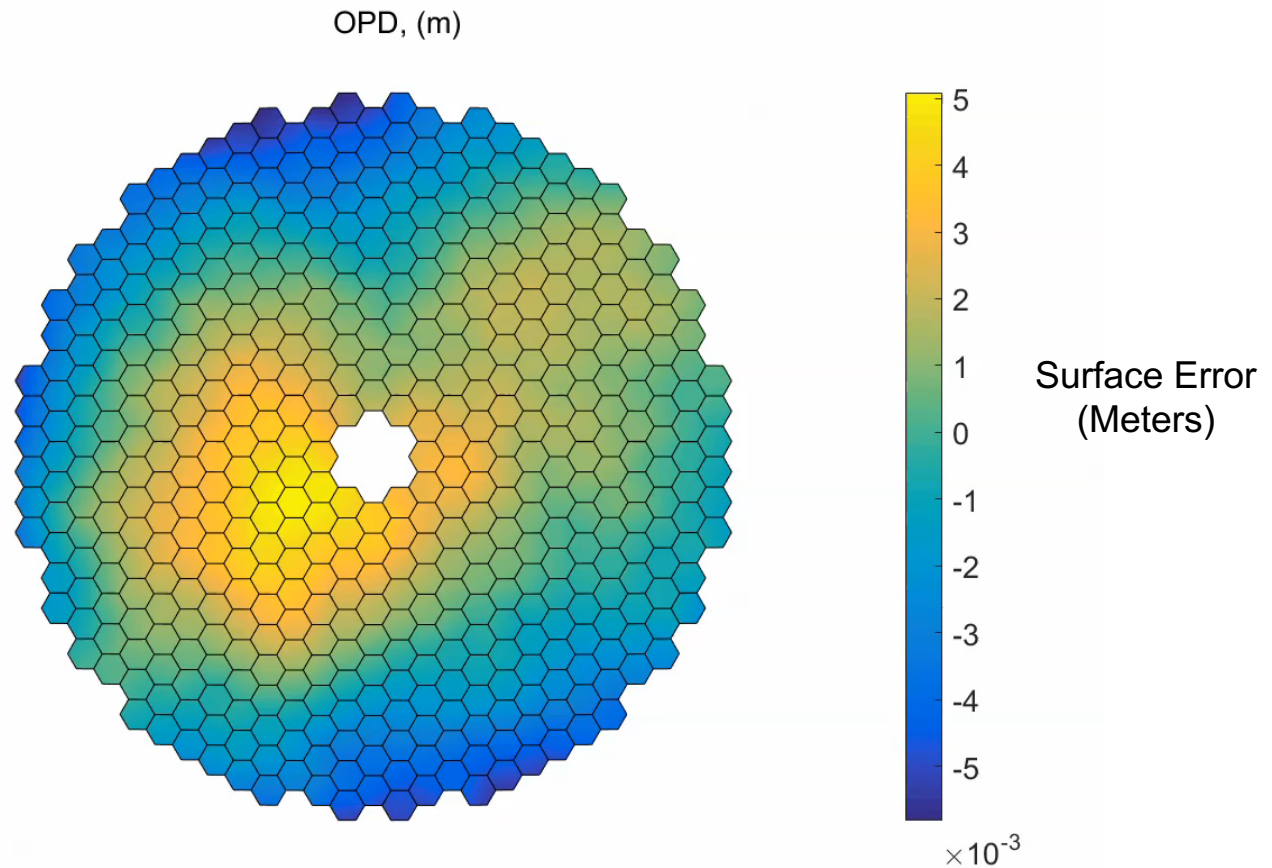
Errors due to clocking are most apparent in rim segments



Includes segment x, y and clocking installation errors,  
but segments are assumed to be perfect

# Simulation Movie

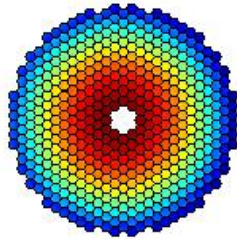
Initial turn-on through phasing, but before warping



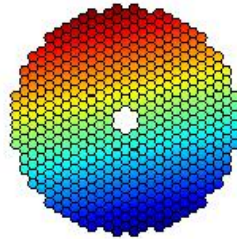
# The First 12 Control Modes

Focus Mode (focus mismatch) is first non-singular control mode, with highest error multiplier

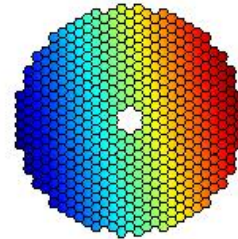
mode 0 err mult 5.686e+004



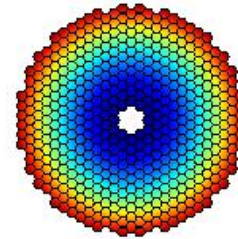
mode 1 err mult 2548.0918



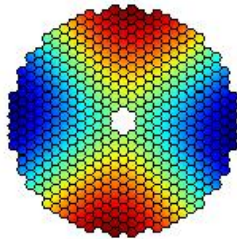
mode 2 err mult 2537.3758



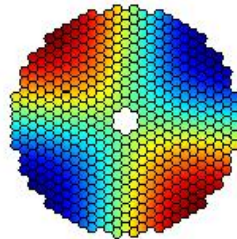
mode 3 err mult 25.4352



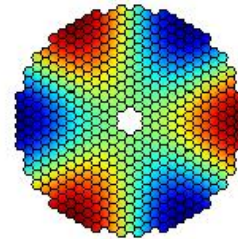
mode 4 err mult 5.0817



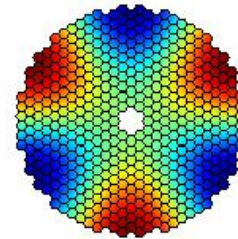
mode 5 err mult 5.0814



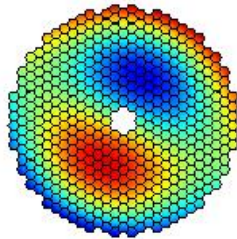
mode 6 err mult 2.2558



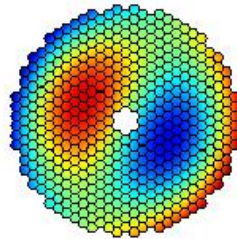
mode 7 err mult 2.2223



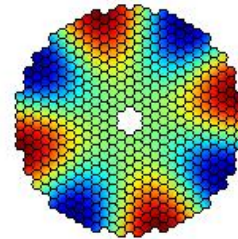
mode 8 err mult 1.9326



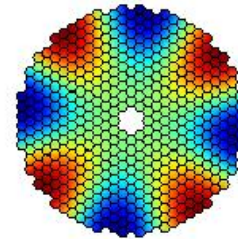
mode 9 err mult 1.9325



mode 10 err mult 1.3457



mode 11 err mult 1.3457



# Focus Mode

Or “Focus Mismatch”

Focus mode is the first non-singular mode of the M1 control system.

In focus mode, the radius of curvature of the surface defined by segment centers does not match the curvature of individual segments, but segment edges remain lined up in height.

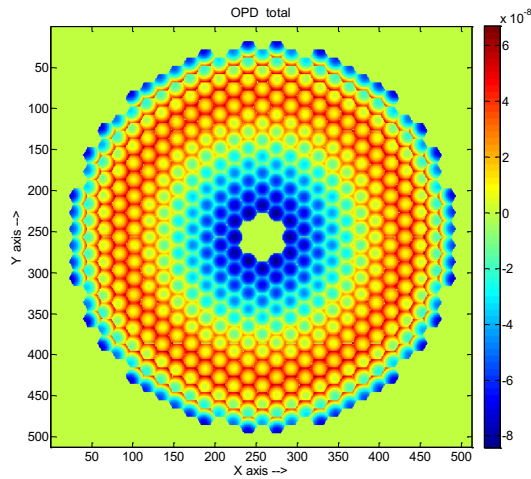
Sensors that only see height find focus mode nearly unobservable, while sensors with dihedral angle sensitivity, that is, non-zero  $L_{\text{eff}}$ , have an error multiplier for focus mode inversely proportional to  $L_{\text{eff}}$ .

Refocusing the telescope by moving M2 reduces the wavefront error due to focus mode by  $\sim N$ , where  $N$  is the number of segments in the mirror.

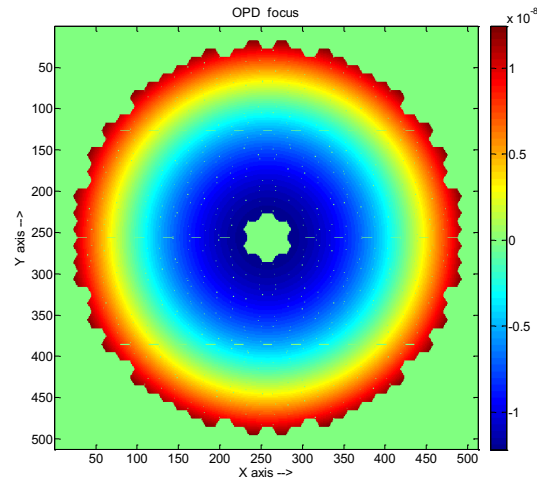
The wavefront residual after refocusing is called “scalloping”, because of its appearance in cross section.

# Correcting 1 $\mu\text{m}$ of M1 Focus Mode ( $\sim 0.8$ nm correlated sensor drift) by Pistoning M2

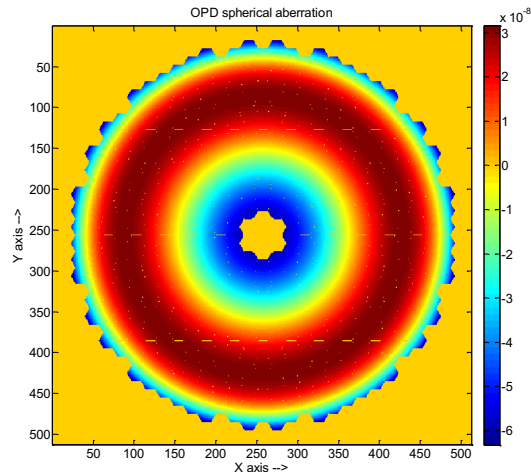
Total  
OPD  
140nm pv



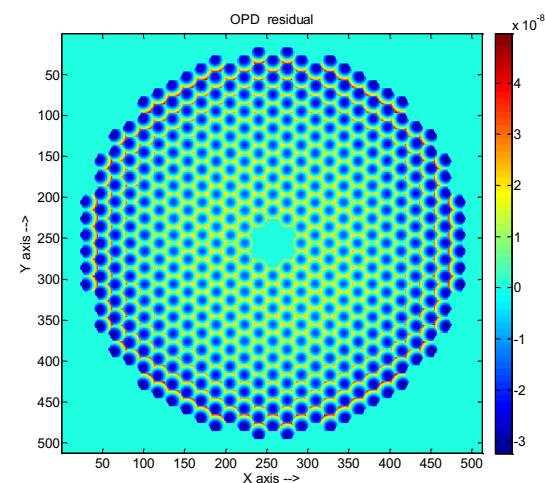
Focus  
OPD  
24nm pv



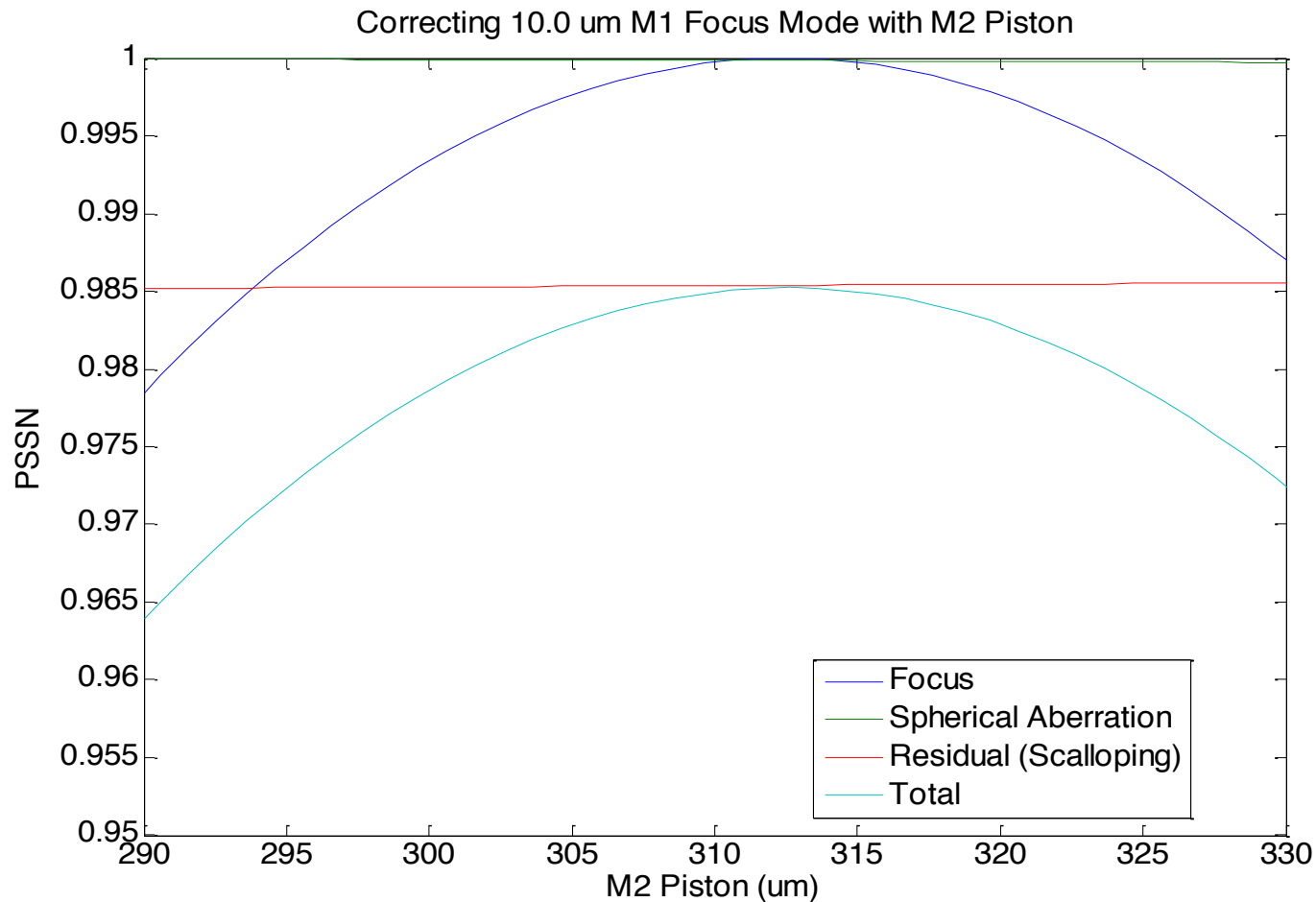
Spherical  
Aberration  
OPD  
90nm pv



Residual  
OPD,  
mostly  
focus-mode  
Scalloping  
75nm pv



# Correcting 10 $\mu\text{m}$ of Focus Mode ( $\sim 8$ nm correlated sensor drift) by Pistoning M2



# Focus Mode

## Implications for Edge Sensors

Any collective drift from any source of all edge sensor height readings together, maps directly to focus mode, with a high multiplier.

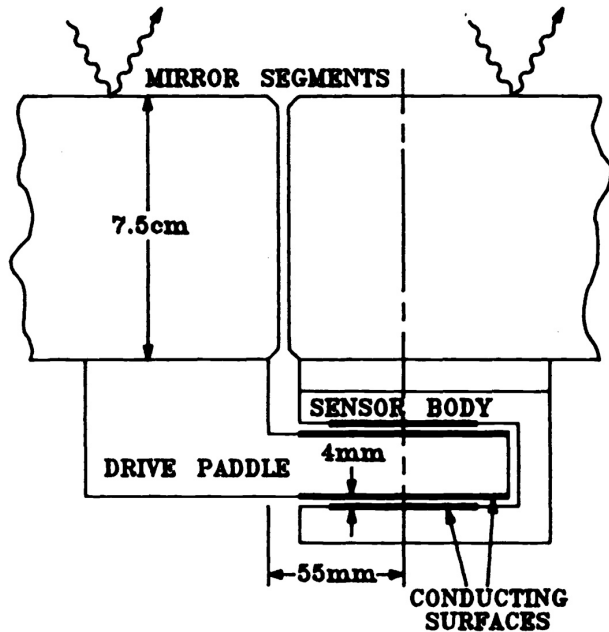
Even with refocusing, focus mode is difficult to control, and there are therefore requirements on  $L_{eff}$  and edge sensor temperature coefficient and long-term stability.

On TMT, the NFIRAOS AO system can estimate focus-mode and thus provide optical correction. This is done with a matrix multiply on WFS data, rather than actuator positions, in which focus mode is unobservable.

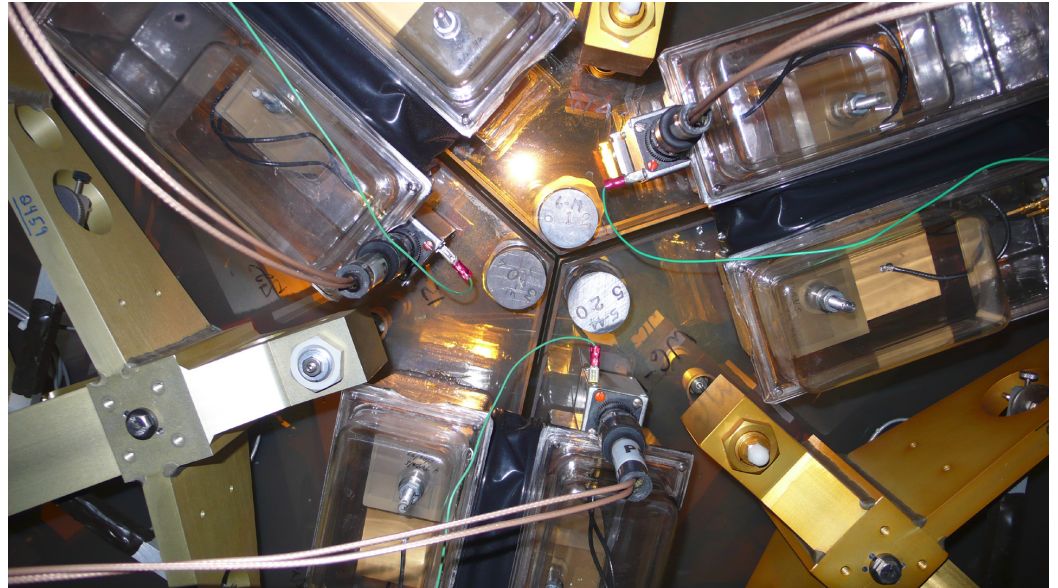
# Keck Edge Sensors

# Keck Edge Sensor

## Sensor Geometry and Appearance



$L_{eff} = 55\text{mm}$



Edge Sensors where three segments meet. The green wires carry ground between drive and sense. On TMT, sensor housings have spring contacts to carry ground.

# Keck Edge Sensors

## Requirements and Performance

	ACS DERIVED REQUIREMENTS	MEASURED PERFORMANCE
<b>SYSTEM REQUIREMENTS</b>		
sensor "noise"	2.5 nm rms	1 nm rms
measurement precision	3 nm lsb	3 nm lsb
dynamic range	$\pm 12\mu\text{m}$	$\pm 12\mu\text{m}$
temporal drift	6 nm/wk	3.2 nm/wk (system)
temperature effects	$< 3\text{ nm/C}$	2 nm/C (system)
operating range	$2\text{ C} \pm 8\text{ C}$	ok
physical protection	boot	ok
<b>MECHANICAL REQUIREMENTS</b>		
gravity	9 nm rms - after correction	7.5 nm rms - after correction
temporal drift	3 nm/wk	3.2 nm/wk (system)
temperature effects	$< 3\text{ nm/C}$	1.5 nm/C
mass	$< 3\text{ kg}$	2 kg
serviceability	for mirror removal	ok
intersegment motion	4.6 nm rms - after correction	4.5 nm rms - after correction
offset	$< \pm 160\mu\text{m}$	$< + 180\mu\text{m}$
<b>ELECTRONIC REQUIREMENTS</b>		
power	$< 2\text{ W}$	$< 0.5\text{ W}$
noise	$< 2.5\text{ nm rms system}$	$< 0.5\text{ nm rms}$
electronic stability	$< 3\text{ nm/wk}$	0.3 nm/wk

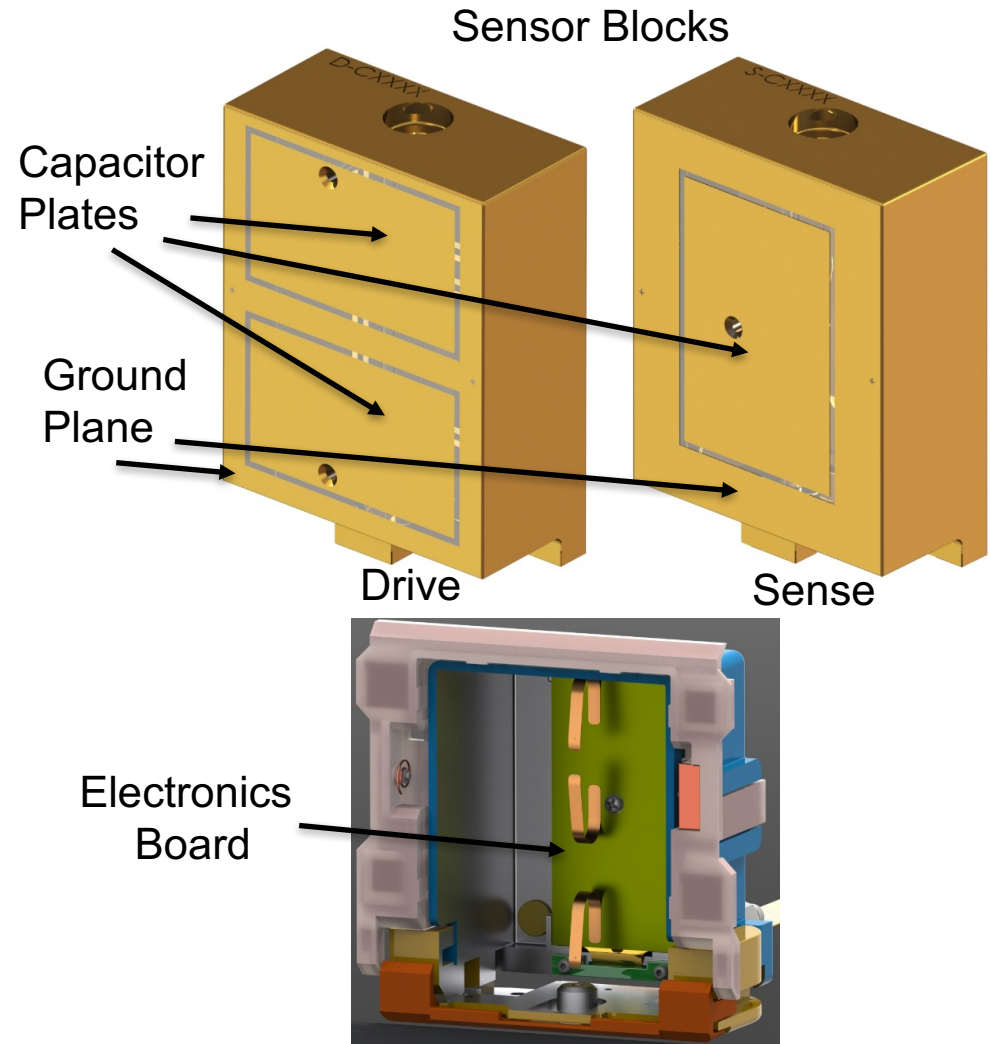
### Displacement sensors for the primary mirror of the W.M. Keck telescope

R.H. Minor, A.A. Arthur, G. Gabor, H.G. Jackson, R.C. Jared, T.S. Mast and B.A. Schaefer  
 SPIE Vol. 1236 Advanced Technology Optical Telescopes IV (1990) /1017

# TMT Edge Sensors

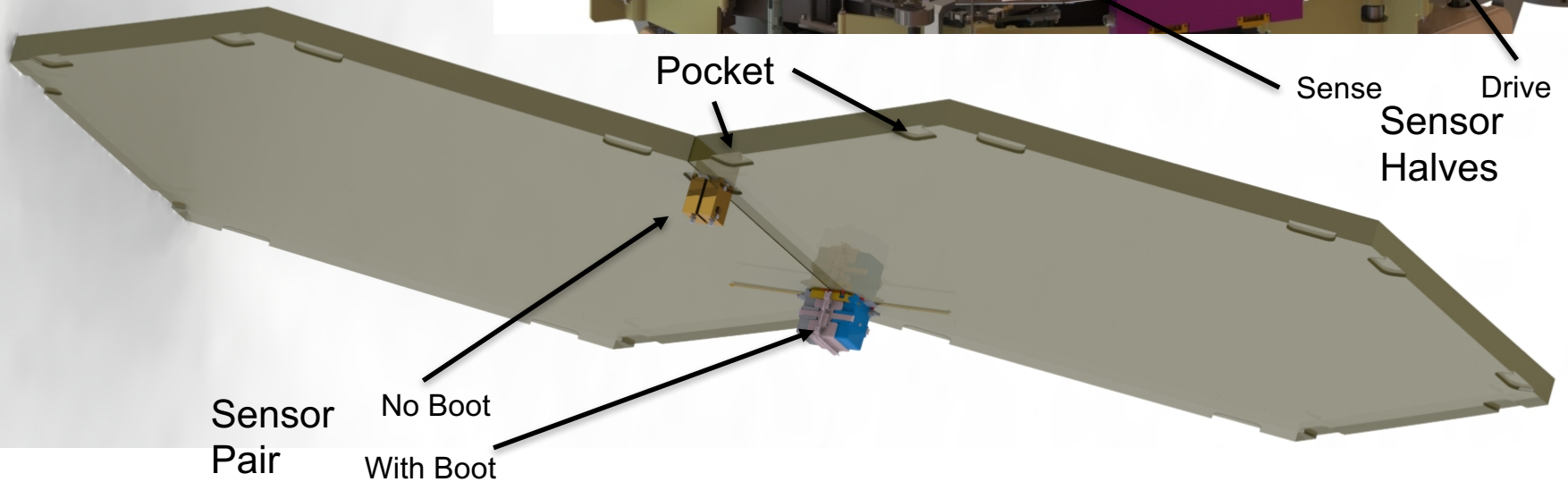
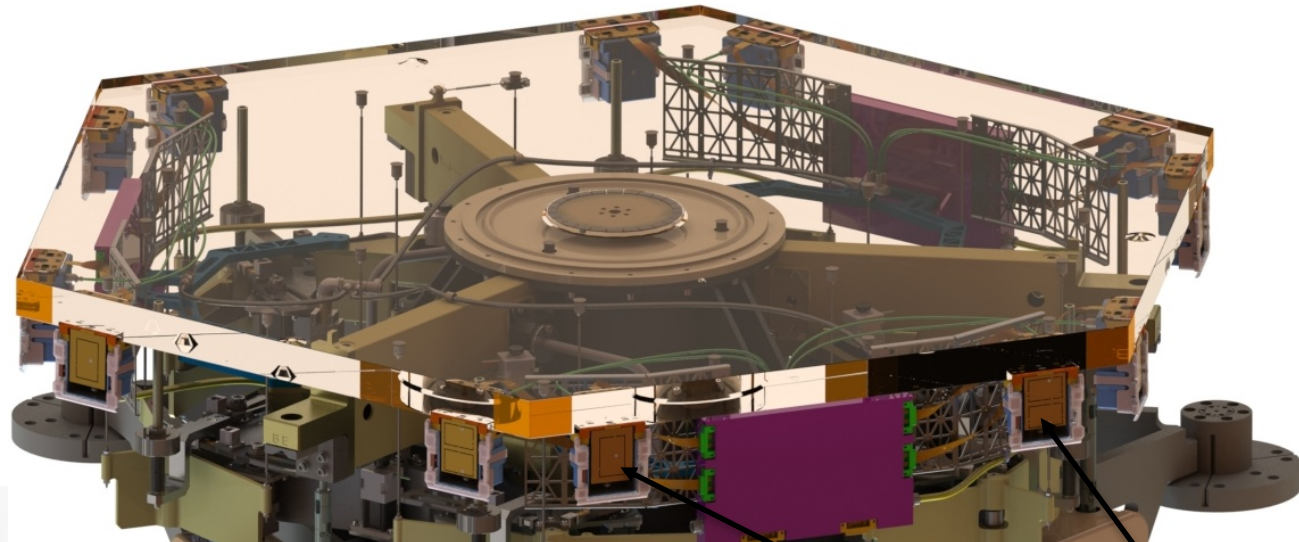
# Sensor Basics

- ◆ There are 2772 sensors on 492 mirrors
  - also 462 sensors mounted on the 82 spares
- ◆ Each sensor consists of
  - Two types of clearceram sensor blocks
    - ◆ Drive (2 plates)
    - ◆ Sense (1 plate)
  - Electronics
  - Protective boot
- ◆ These two blocks together with their electronics and boots form a complete sensor
- ◆ The sensors provide two outputs which measure the physical relationship between the blocks
  - Relative gap
  - Relative height (height + constant\*gap)
- ◆ Together the 2772 gap and height measurements drive the control system.



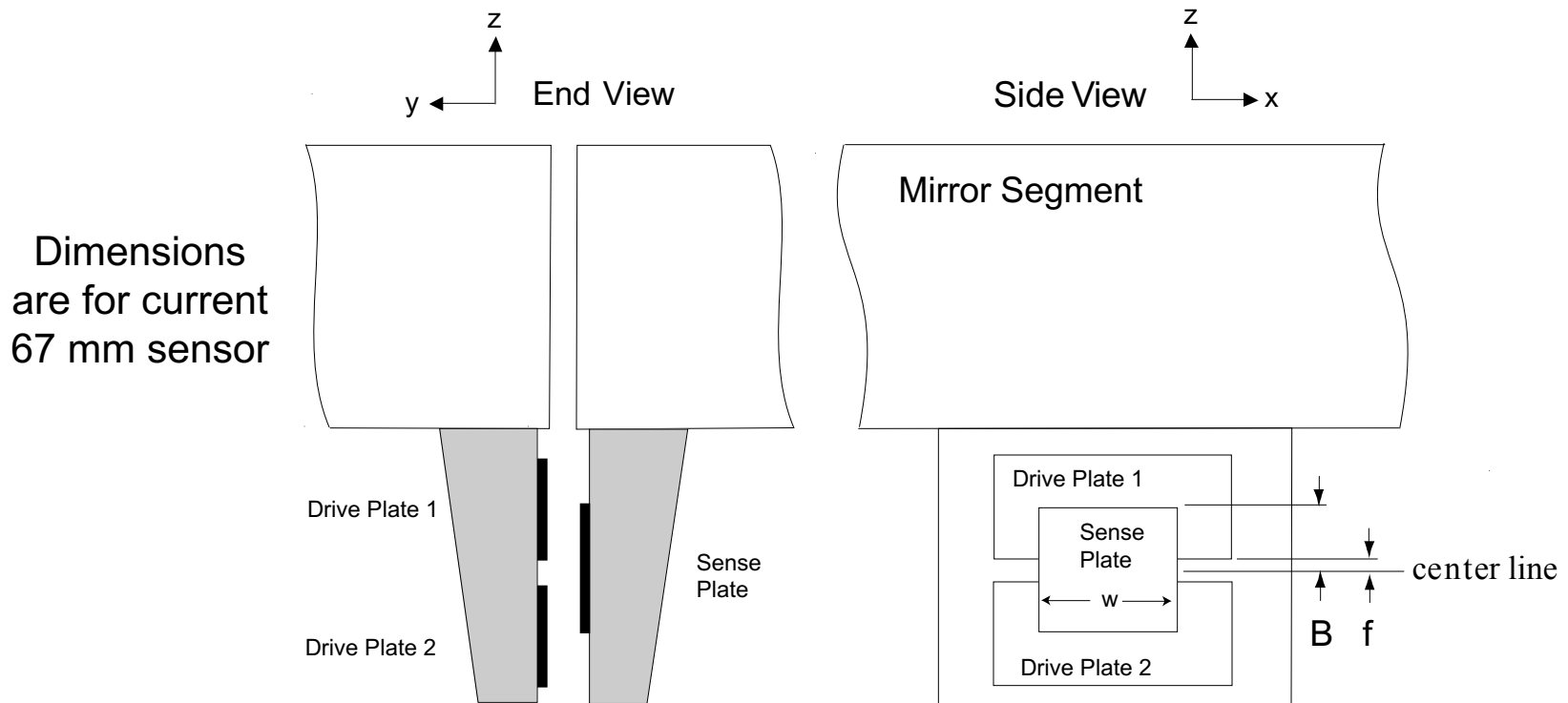
# Sensor Locations

- ◆ Sensor feet directly contact the back of the mirror in flat pockets
- ◆ Sensor is anchored by puck which is bonded to mirror



# TMT Edge Sensor

Capacitive, face-on geometry, height/tilt output and gap output



- $w$  Sense plate effective width (30 mm)
- $2B$  Sense plate effective height (45 mm)
- $2f$  Effective spacing between drive plates (6 mm)
- $V$  Drive amplitude (0 to 8.192 Vpp)

# TMT Edge Sensor

## Analytic Model

$$R = \frac{A}{y} \left( k(B - f) - z - x\theta_y + \frac{B^2 - f^2}{2y} \theta_x \right)$$

$$A = \epsilon_0 w V \quad \text{Square wave excitation}$$

$$A = 2\pi f_s \epsilon_0 w V \quad \text{Sine wave excitation}$$

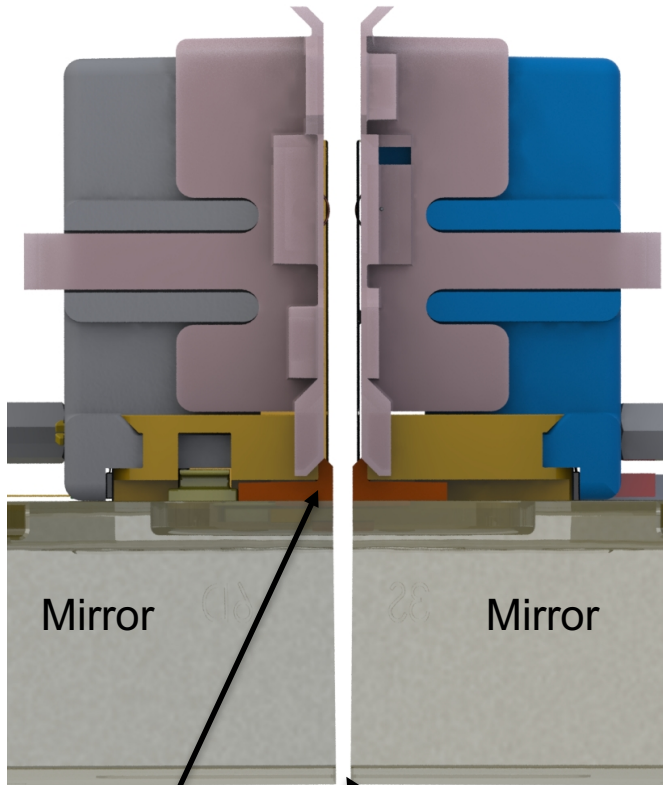
$$L_{eff} = \frac{B^2 - f^2}{2y}$$

R	Sensor reading (coulombs for square wave, amperes for sine wave)
$\epsilon_0$	8.854 10-12 farads / meter
w	Sense plate effective width (30 mm)
2B	Sense plate effective height (45 mm)
2f	Effective spacing between drive plates (6 mm)
y	Gap from drive to sense (4.8 +/- 1.0 mm)
V	Drive amplitude (0 to 8.192 Vpp)
fs	Drive frequency
	Drive-side tip and tilt as seen from sense side
x,y,z	Coordinates of drive side as seen from sense side
k	= (Common-mode drive amplitude)/(Differential drive amplitude)

# TMT Edge Sensors

Sensor housings allow hands-off segment installation and removal

Moving Shell retracted



Snow Blockers separated

0 mm to 4.5mm

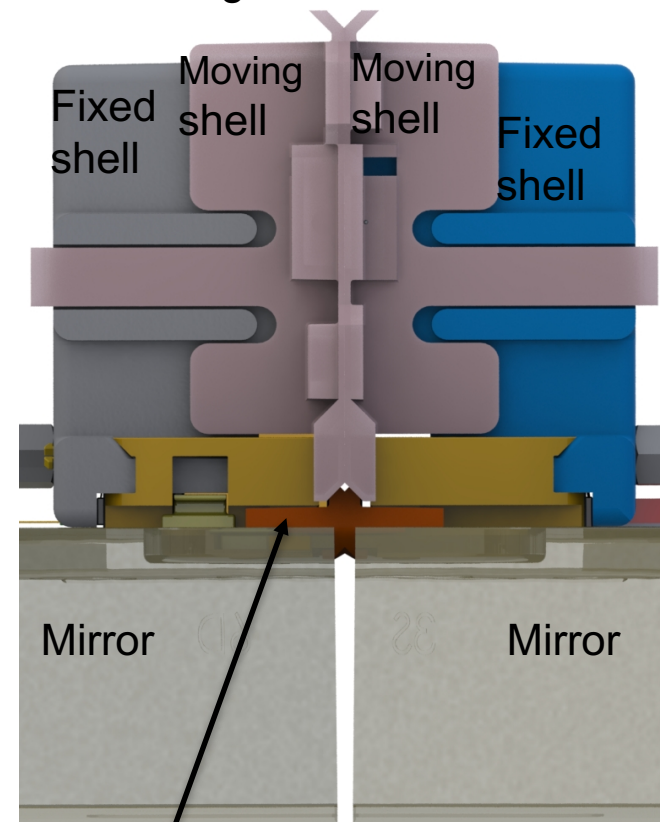
◆ Sensor boots bridge the intersegment gap

- Dust and purge seal
- Ground
- CO2 snow protection
- EMI Protection

◆ Gap 2.5mm nominal

- May Go to 0 during segment removal (a  $3\sigma$  event)
- Operational range  $\pm 2\text{mm}$
- Drives snow blocker design

Moving Shell Connected



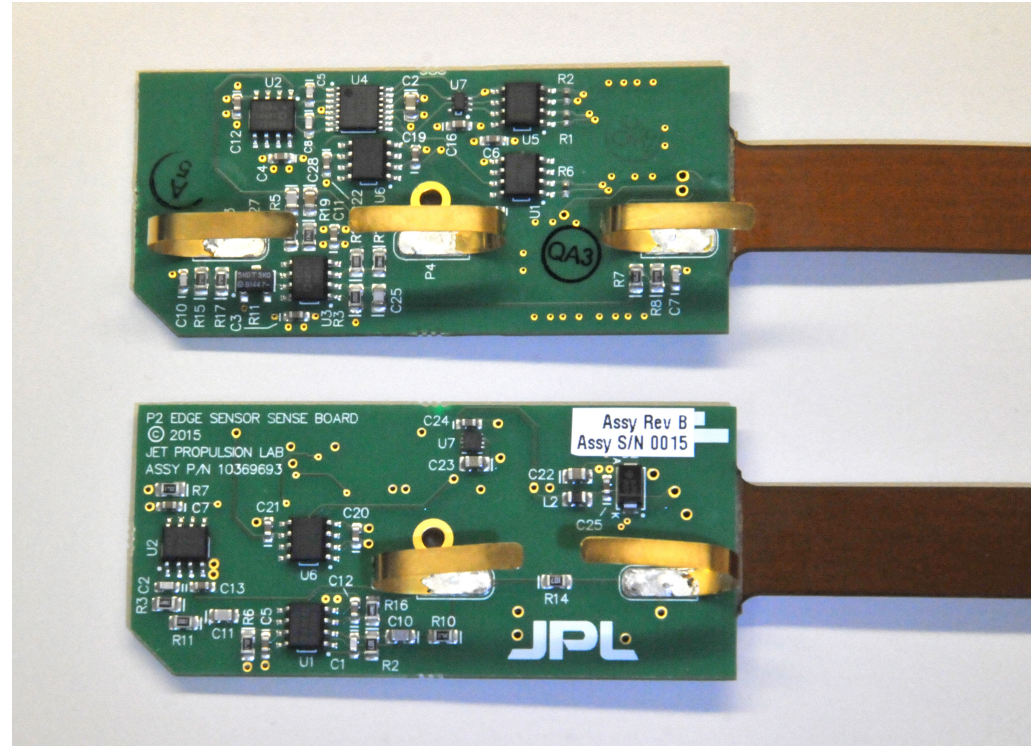
Snow Blockers connected

# TMT Edge Sensors

Drive and Sense Electronics

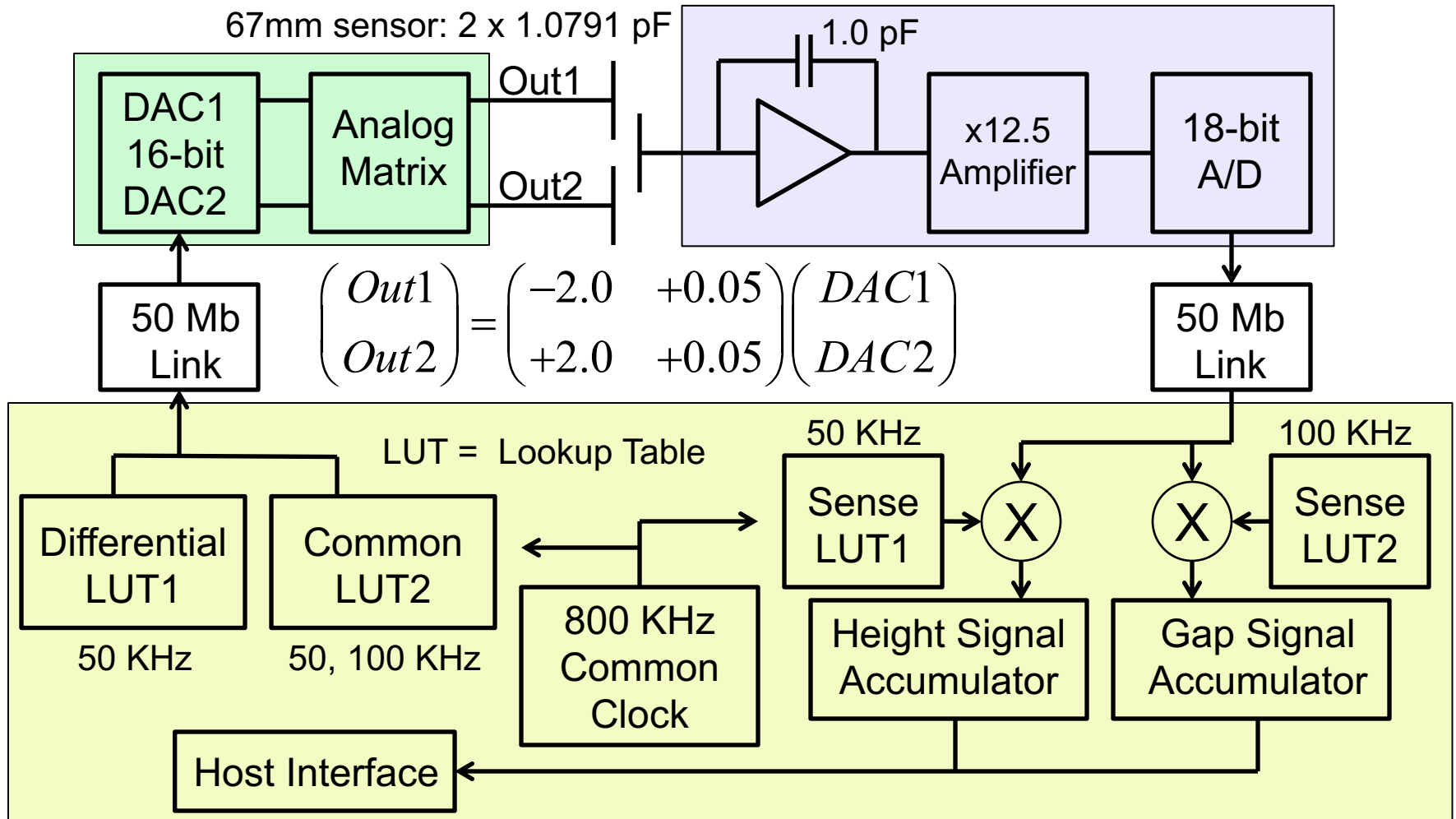
Boards are  
30x65 mm

Flex is  
12x330 mm



# TMT Edge Sensors

## Electronics Block Diagram



# TMT Edge Sensors

## Performance Summary

Version 2 (V2) electronics have been fully tested. V3 electronics are now in test, are expected to improve the following numbers, particularly the temperature coefficient.

Height noise density: Requirement is  $2.8 \text{ nm}/\sqrt{\text{Hz}}$ , measured is  $2.2 \text{ nm}/\sqrt{\text{Hz}}$ . The V3 electronics should improve this somewhat.

Height temperature coefficient: Requirement is  $1 \text{ nm}/\text{C}$  after calibration. The V2 electronics were measured at  $12 \text{ nm}/\text{C}$  before calibration, which meets the post-calibration requirement with little margin. The V3 electronics, now being evaluated, should give much more margin.

Power dissipation: Requirement is  $200 \text{ mW}$  or less. Actual drive board power is  $99.2 \text{ mW}$ , sense board is  $90.5 \text{ mW}$ , total is  $190 \text{ mW}$ .

# Edge Sensor Calibration

The TMT M1 edge sensors need to resolve 5 nm height differences in the presence of “in-plane” motions spanning a millimeter.

If this is taken at face value, the sensors must be installed with an angular accuracy of 5 nm / 0.5 mm, or 10  $\mu$ rad.

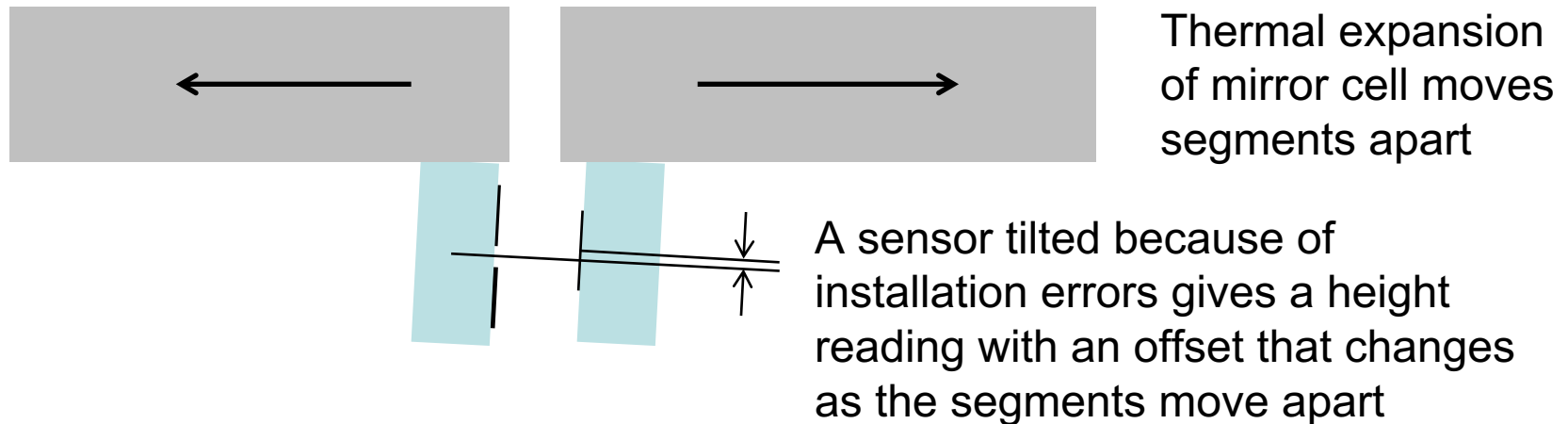
Terry Mast, Jerry Nelson and Gary Chanan proposed in 2007 to use edge sensor gap readings to measure in-plane motions, and to use this knowledge plus telescope phasing (APS) runs on bright stars to “calibrate” the as-installed sensors.

“Calibration” corrects edge sensor readings for in-plane motions, relaxing sensor installation tolerances. For TMT, a 10  $\mu$ rad tolerance becomes an attainable 450  $\mu$ rad tolerance.

EELT’s inductive, face-on, sensor has similar interactions with in-plane motions. EELT uses gap and shear measurements to correct sensor readings.

The Keck capacitive, interleaved, geometry is less sensitive to in-plane motions, and sensors were manually measured and shimmed to alignment. Keck calibration consists of a set of lookup tables of sensor setpoints vs zenith angle, without considering in-plane motions.

# An Example of the Need for Calibration



- ◆ Consider ordinary thermal expansion of the steel M1 support structure vs that of the zerodur mirror segments. By itself this gives a change in the gap between segments of  $14.4 \mu\text{m}/\text{C}$ .
- ◆ If an edge sensor is mounted onto the mirror segments with a  $1 \text{ mrad}$  tilt, that edge sensor now has a  $14.4 \text{ nm}/\text{C}$  height error, but the need is for  $1 \text{ nm}/\text{C}$  or less, after calibration.

# TMT Performance Metrics

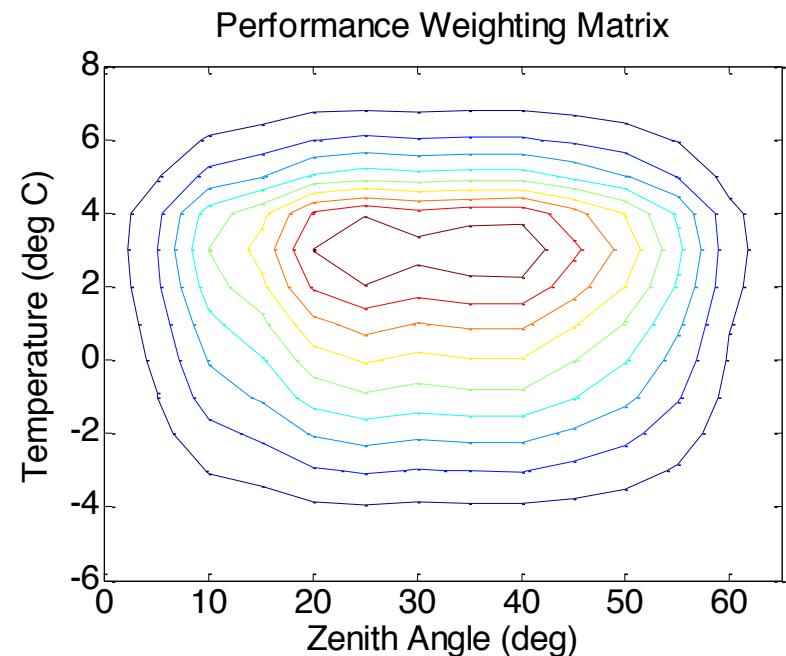
## PSSN and the Standard Year

The TMT figure of merit for seeing-limited observations is Point Source Sensitivity, Normalized, or PSSN [Ref 18].

The TMT Standard Year [Ref 13] is a record of Mauna Kea temperatures and Gemini North pointing from 6/29/2006 to 6/1/2008.

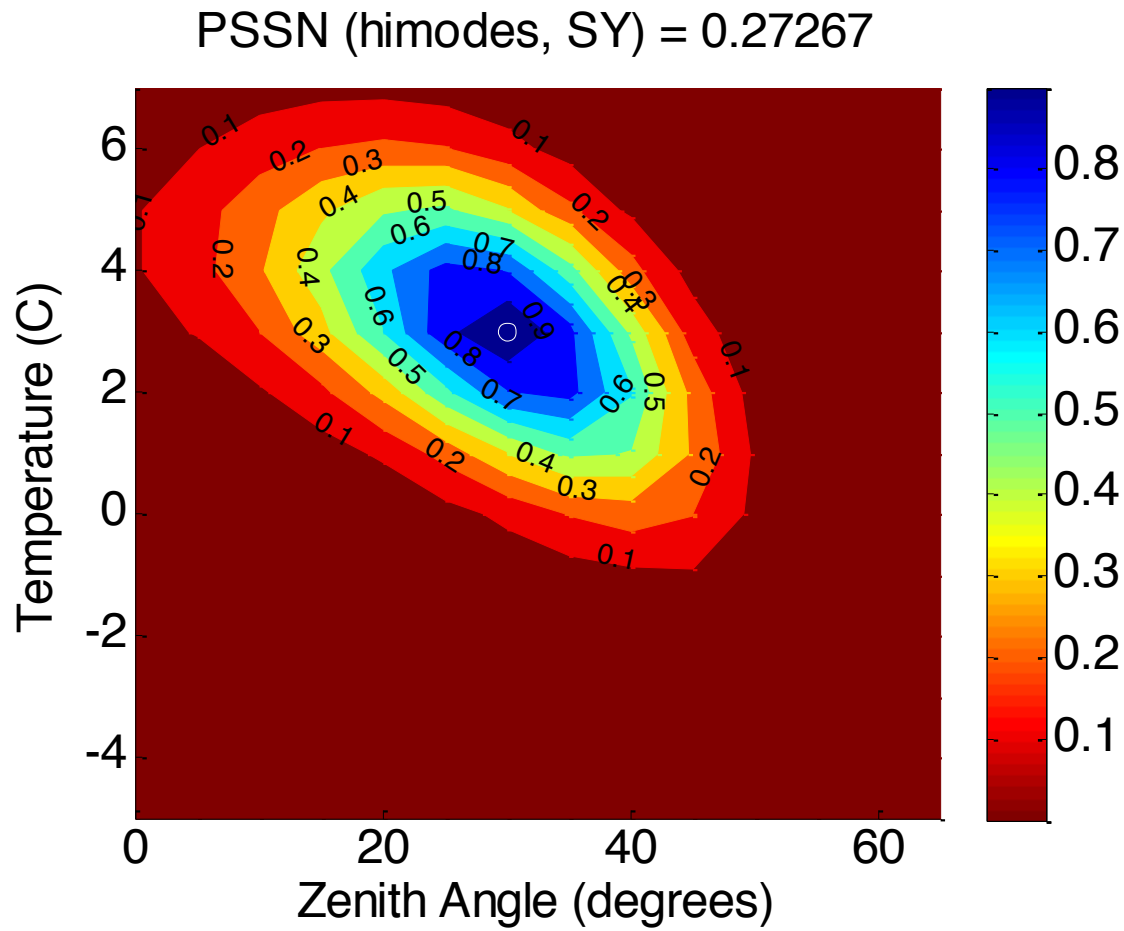
A performance weighting matrix (shown) was computed from the Standard Year record.

Edge sensor performance is evaluated and optimized using PSSN averaged with Standard Year weighting



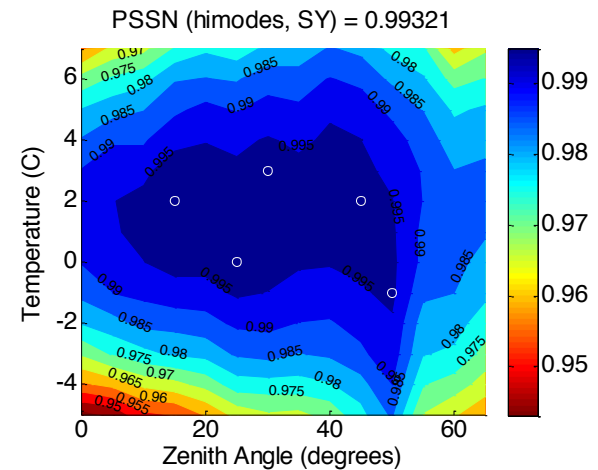
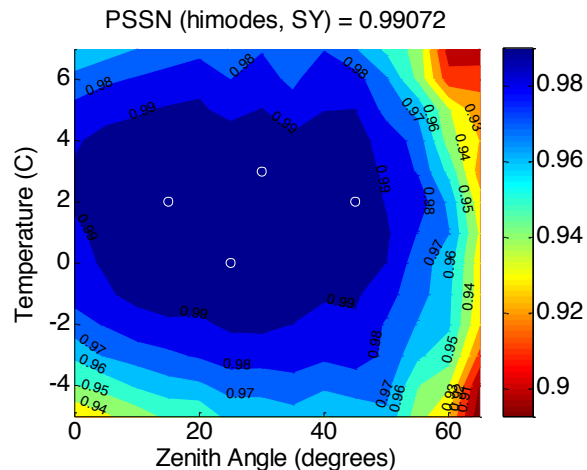
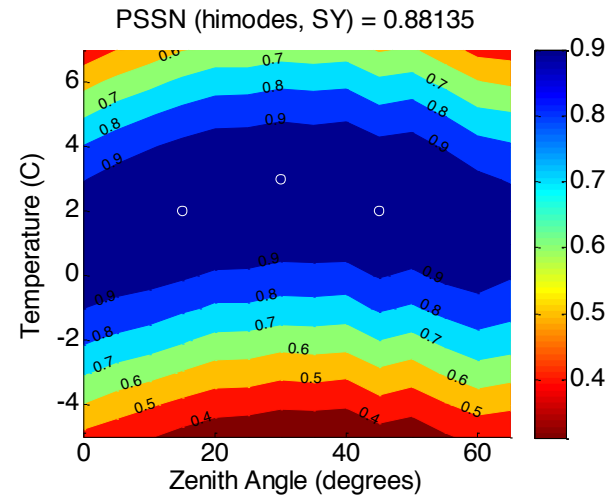
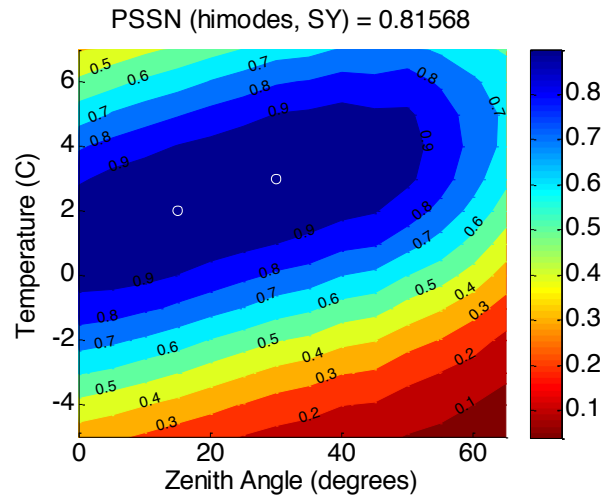
# The Need for Calibration

## PSSN vs Zenith Angle and Temperature for 1 APS Run



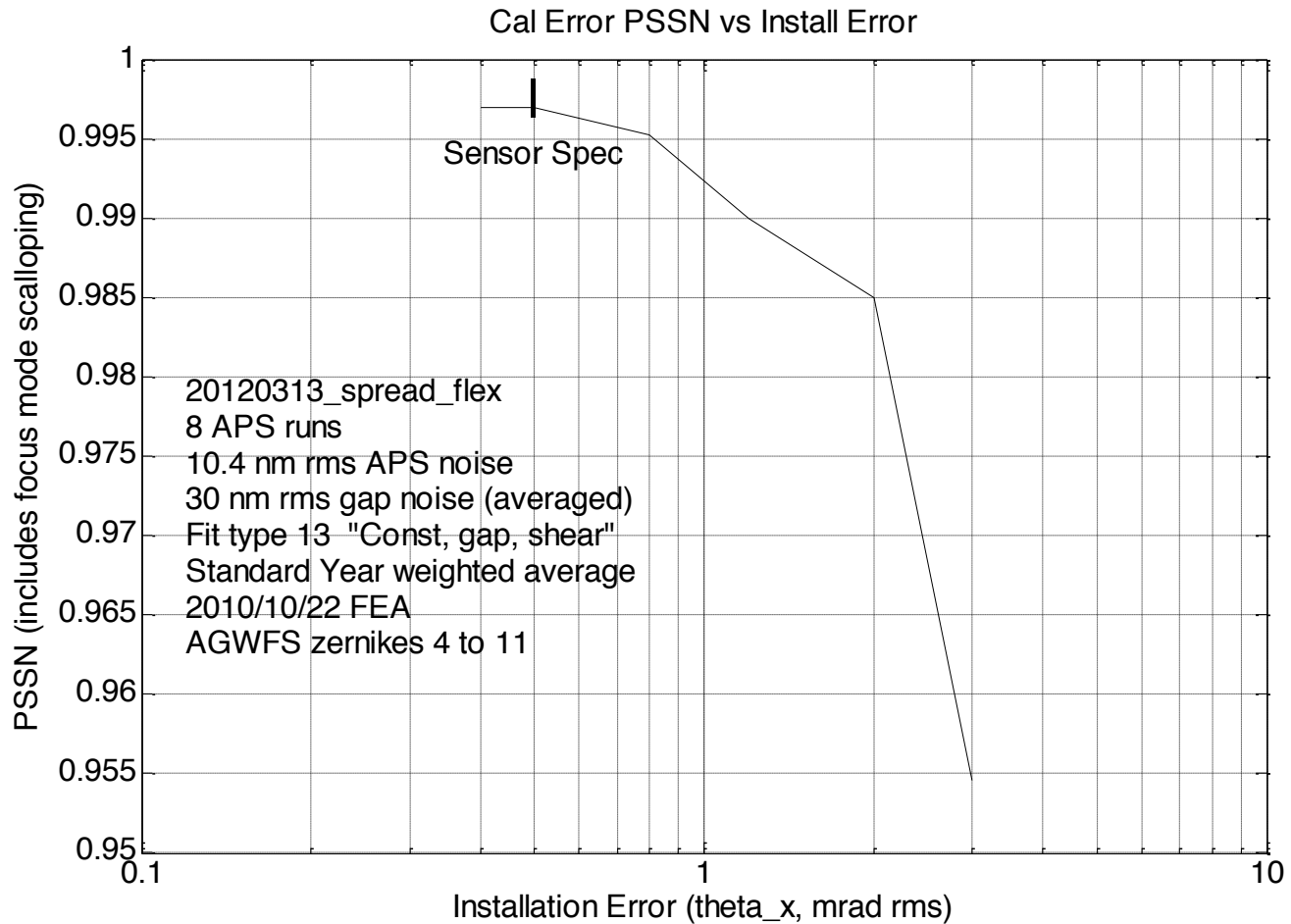
# Calibration Results

## PSSN vs Zenith Angle and Temperature for 2-5 APS Runs



# TMT Edge Sensor

## Calibration PSSN vs Installation Error



# E-ELT Edge Sensors

# E-ELT Edge Sensors

## Overview

The E-ELT edge sensors are face-on like TMT, but are inductive rather than capacitive.

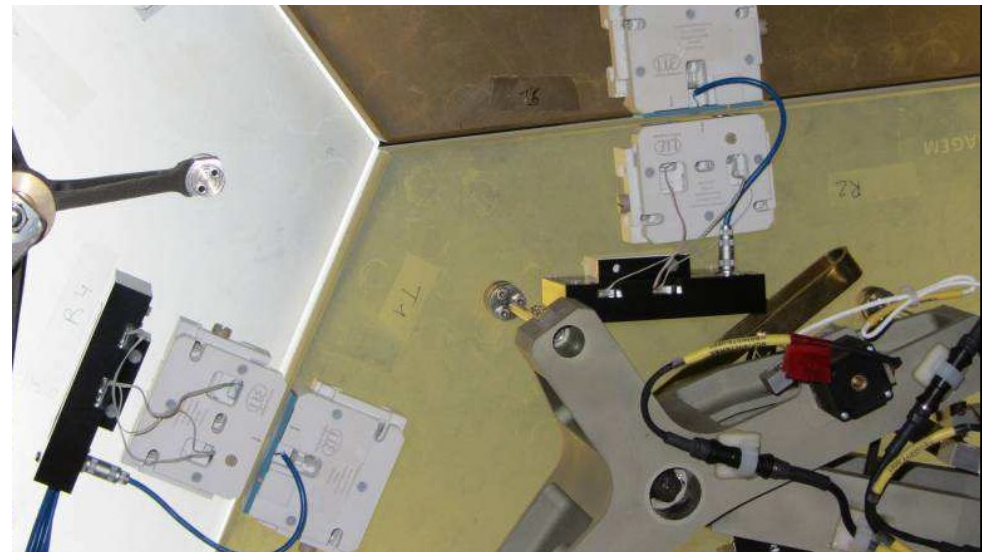
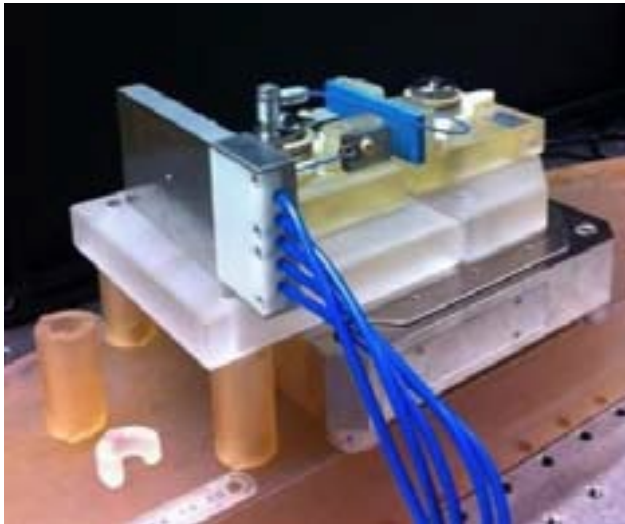
They use an innovative approach to coil stability where conducting traces are embedded in ceramic, and the assembly is fired together to make a low-temperature-coefficient ceramic block. The sensor inductive properties have the tempco of the ceramic block.

This 2014 SPIE paper describes the E-ELT edge sensors:

Wasmeier, M., Hackl, J., Leveque, S., “Inductive sensors based on embedded coil technology for nanometric inter-segment position sensing of the E-ELT,” *Proc. of SPIE* Vol. 9145, 91451R-1 (2014).

# E-ELT Edge Sensors

## Prototypes under test



# E-ELT Edge Sensors

**Performance Requirements – These have been met**

Nominal gap 4mm

$L_{\text{eff}} = >10 \text{ mm}$

Piston (height/tilt)

Noise  $<1 \text{ nm/rHz}$

Drift  $<10 \text{ nm / week}$  at constant temperature, humidity

Span  $\pm 200\mu\text{m}$

Gap

Noise  $<100 \text{ nm/rHz}$

Drift  $<200 \text{ nm/week}$  at constant temperature, humidity

Span  $\pm 1 \text{ mm}$

Shear

Noise  $<100 \text{ nm/rHz}$

Drift  $<100 \mu\text{m/week}$  at constant temperature, humidity

Span  $\pm 1 \text{ mm}$

# Backup Material

# The 6 Degree-of-Freedom A-Matrix

# The 6 Degree-of-Freedom A-matrix

- The 6DOF A-matrix express how segment motions in all six degrees of freedom affect edge sensor height, gap and shear.
- Segment out-of-plane motions are tip, tilt and piston. These are controlled by actuators.
- Segment in-plane motions are inplane\_X, inplane\_Y and clocking. These are caused by gravity deformation and temperature changes, plus initial in-plane positions are subject to segment installation errors.

$$\begin{pmatrix} \textit{height} \\ \textit{gap} \\ \textit{shear} \end{pmatrix} = A_{6DOF} \begin{pmatrix} \textit{tip} \\ \textit{tilt} \\ \textit{piston} \\ \textit{inplane\_X} \\ \textit{inplane\_Y} \\ \textit{clocking} \end{pmatrix}$$

# The Need for the 6DOF A-matrix

- The 6 DOF A-matrix plays a major role in analyzing calibration, control stability and focus mode, in comparing TMT and ESO methodology, and is necessary for the gap-to-shear transformation.
- The 6 DOF A-matrix provides a rigorous 3-D model of the M1 geometry for controls analysis.
- It has a full set of inputs:
  - Ideal M1 geometry
  - Merit-Function-generated segment, vertex, sensor and actuator locations and orientations
  - Gravity deformations
  - Temperature expansion
  - Segment installation error
  - Sensor installation error
  - Sensor gravity flexure
  - Sensor temperature coefficient

# The Parts of the 6DOF A-Matrix

Standard 3D A-Matrix →	Height per actuator stroke	Height per inplane X, Y	Height per segment clocking	
	Gap per actuator stroke	Gap per inplane X, Y	Gap per segment clocking	← G Matrix
	Shear per actuator stroke	Shear per inplane X, Y	Shear per segment clocking	← H Matrix

The 6 DOF A-matrix is created by moving each segment slightly in each of its 6 degrees of freedom, while observing the effect on sensor height, gap and shear readings.

# Computing Shears from Gaps

# Obtaining Shear Data

- Calibration of face-on edge sensors requires a knowledge both of gap and shear aspects of the in-plane segment motions. The TMT baseline sensor provides a gap output, but not a shear output.
- Shear data can be measured with shear sensing (ESO approach), or computed from gap data (TMT approach).
- The procedure for computing shears from gaps [Ref 15] is summarized in the next slide. It uses the G and H matrices defined in the A-matrix discussion.
- The procedure works well, and has the side benefit of filtering out the unphysical part of gap noise. In simulation, the measured noise multiplier agrees with the theoretical value.

# Computing Shears from Gaps

- Gap readings, called here  $y_{\text{measured}}$ , can be turned into best-fit sensor x (shear) and y (gap) offsets as follows --

$$x_{\text{calculated}} = HG^{\dagger} y_{\text{measured}}$$

$$y_{\text{calculated}} = GG^{\dagger} y_{\text{measured}}$$

- G is a constant matrix connecting segment coordinates to sensor-y coordinates.  $G^{\dagger}$  is the pseudo-inverse of G. H connects segment coordinates to sensor-x coordinates.
- For details, see Gary Chanan, “Segment In-Plane Position Sensing”, TMT.CTR.PRE.07.019.REL01 (2007) [Ref. 12].

# TMT and ESO Focus Mode Approaches (Doug McMarten)

- ESO measures piston, shear, and gap (PSG) with each sensor
  - ESO does not use dihedral sensitivity
  - Shear and gap are used to
    - Provide a (quasi-static) initial estimate for focus-mode amplitude
    - Provide full knowledge of in-plane gap and shear for calibration
- TMT requires only (i) piston +  $(L_{\text{eff}}) \times$  (dihedral) and (ii) gap
  - Dihedral provides better (less noisy) estimate of focus-mode than PSG
    - We can also estimate focus-mode scalloping with AO, so AO can be used to correct any correlated sensor drift between APS runs.
  - Shear can be estimated from gap
    - Noise multiplier = 2.23
    - One unobservable mode (torsion)
      - Amplitude of this mode is believed to be negligible
      - Could be observable with one or a few shear sensors

# References

1. R.H. Minor, A.A. Arthur, G. Gabor, H.G. Jackson, R.C. Jared, T.S. Mast and B.A. Schaefer, "Displacement sensors for the primary mirror of the W.M. Keck telescope," *Proc. SPIE* 1236, 1017 (1990)
2. D. G. MacMartin, G. A. Chanan, "Control of the California Extremely Large Telescope primary mirror," *Proc. SPIE* 4840, 69-80 (2003).
3. Chanan, G., MacMartin, D.G., Nelson, J., and Mast, T., "Control and Alignment of Segmented-Mirror Telescopes: Matrices, Modes and Error Propagation", *Applied Optics*, Vol 43, No. 6, 1223-1232 (2004).
4. Roberts, S., Sun, S., Kerley, D., "Optical performance analysis and optimization of large telescope structural designs", *Proc. SPIE* 5867, 200-211 (2005).
5. Mast, T., Chanan, G., Nelson, J., Minor, R., Jared, R., "Edge sensor design for the TMT," *Proc. SPIE* 6267, 62672S (2006).
6. G. Chanan, M. Troy, I. Crossfield, J. Nelson, and T. Mast, "The Alignment and Phasing System for the Thirty Meter Telescope," *Proc. SPIE* 6267, pp. 62672V (2006).
7. J. Nelson, "Edge Sensors: Abstract view," TMT.PSC.PRE.07.004.DRF01 (2007).
11. Jared, R., Minor, R., Doering, D., Van der Lippe, "Relative Humidity and the TMT Sensor," TMT.CTR.PRE.07.010.REL01 (2007).
12. Gary Chanan, "Segment In-Plane Position Sensing", TMT.CTR.PRE.07.019.REL01 (2007).
13. Vogiatzis, K., "Probabilistic Performance Analysis 'Standard Year'", TMT.SEN.PRE.07.030.DRF01 (2007).
14. Shelton, C., Mast, T., Chanan, G., Nelson, J., Roberts, L., Troy, M., Sirota, M., Seo, B-J., MacDonald, D., "Advances in Edge Sensors for the Thirty Meter Telescope Primary Mirror", *SPIE* 7012-35, 2008.
15. D. Rozière, B. Luong, B. Fuchs, A. Périn, C. Néel, S. Lévêque, "Inductive edge sensors: an innovative solution for ELT segmented mirror alignment monitoring", *Proc. SPIE* 7012, 701217-701217-14 (2008).
16. K. Szeto et al. "TMT telescope structure system: design and development progress," *Proc. SPIE* 7012-88 (2008).
17. M. Troy et al., "A conceptual design for the Thirty Meter Telescope Alignment and Phasing System," *Proc. SPIE* 7012-125 (2008).
18. Seo, B.-J., Nissly, C., Angeli, G., Ellerbroek, B., Nelson, J., Sigrist, N., and Troy, M., "Analysis of Normalized Point Source Sensitivity as performance metric for large telescopes," *Applied Optics* 48, pp. 5997-6007 (2009).
19. Shelton, C., Roberts, L.C., "M1CS Edge Sensor Calibration Analysis III", TMT.CTR.TEC.12.003.REL01 (2012).
20. Wasmeier, M., Hackl, J., Leveque, S., "Inductive sensors based on embedded coil technology for nanometric inter-segment position sensing of the E-ELT," *Proc. of SPIE* Vol. 9145, 91451R-1 (2014).



**Jet Propulsion Laboratory**  
California Institute of Technology

---

[jpl.nasa.gov](http://jpl.nasa.gov)